nature sustainability

Article

https://doi.org/10.1038/s41893-026-01815-w

Methane pyrolysis-enabled production of high-value carbon fibres

Received: 17 December 2024

Accepted: 17 March 2026

Published online: 16 April 2026

Check for updates

Tangyuan Li[1,2,12], Canhui Wang[3,4,12], Cliff A. Wood[5,12], Kaizhu Zeng[1,2,12], Qi Dong[2], Matthew Gonzalez[6], Bodiuzzaman Jony[5], Sichao Cheng[7], Xinpeng Zhao[2], Alexandra H. Brozena[1,2], Kishor Gupta[5], Pedro J. Arias-Monje[5], Xin Zhang[2], Keenan J. Mintz[5], Han Zong[3], Shen Wang[6], Xizheng Wang[2], Hongmei Gu[8], Dongxia Liu[7], Ping Liu[6], Satish Kumar[5] ✉, Chao Wang[3,9] ✉ & Liangbing Hu[1,2,10,11] ✉

Carbon fibres (CFs) are indispensable for lightweight structural engineering, yet their widespread adoption is stifled by the high cost and environmental toll of polyacrylonitrile (PAN) precursors. While substituting PAN with low-footprint alternatives such as lignin or carbon black reduces emissions, the resulting fibres typically suffer from mechanical degradation caused by poorly integrated fillers. Here we report an electrified carbon-fibre upgrading strategy that transforms low-cost, carbon-black-loaded PAN precursors into high-performance CFs by incorporating methane (CH_4)-derived carbon. By using a porous, aligned fibril network as a Joule-heating element, we achieve rapid, high-temperature pyrolysis at 1,700 K that drives CH_4 diffusion and densification of the internal microstructure. The resulting upgraded carbon fibres, comprising ~50 wt% CH_4-derived carbon, exhibit a tensile strength of 1.7 GPa and a modulus of 173 GPa. This electrified synthesis simultaneously slashes production costs to ~US$13.52 kg_{CF}^{-1} and carbon footprints to ~22.39 kg_{CO2} kg_{CF}^{-1}, offering a commercially viable pathway for high-volume industries such as automotive manufacturing. Our findings establish a circular carbon economy model that converts greenhouse gases into high-value structural materials while yielding hydrogen as a clean coproduct.

Carbon fibres (CFs) have become indispensable to high-end aerospace and performance engineering, prized for their exceptional specific strength and modulus[1–3]. Despite their critical importance, the global CF market remains overwhelmingly dominated by polyacrylonitrile (PAN)-derived precursors, which account for over 90% of commercial production[4]. However, the prohibitive cost and environmental footprint of PAN-based CFs preclude their universal adoption in high-volume sectors such as wind energy and automotive manufacturing[5,6]. To address this, the US Department of Energy (DOE) has established a benchmark for 'affordable' CFs—targeting a cost of US$11.0–15.0 kg_{CF}^{-1} with a threshold tensile strength and modulus of 1.7 GPa and 170 GPa, respectively—to catalyse their integration into mass-market vehicle production[7]. At present, these economic and ecological barriers stem primarily from the high price of PAN precursors and the energy-intensive thermal transformation required during oxidative stabilization and carbonization[5,8]. Developing a pathway that bypasses these constraints remains a central challenge in the transition towards a sustainable, CF-reinforced economy.

To address these economic barriers, research has focused on cost-effective precursors to partially or fully displace PAN[5,9,10]. Sustainable alternatives, such as lignin and carbon black (CB), have been integrated as low-footprint fillers[11–14]; however, the resulting composites

A full list of affiliations appears at the end of the paper. ✉e-mail: satish.kumar@mse.gatech.edu; chaowang@jhu.edu; liangbing.hu@yale.edu

exhibit poor mechanical properties. These performance losses stem from unbound fillers which function as structural defects within the PAN-derived carbon matrix, preventing these materials from meeting the rigorous benchmarks set by the US DOE[7]. For instance, lignin/PAN CFs containing 50 wt% lignin achieve only ~1.2 GPa in tensile strength and ~130 GPa in modulus, whereas CB/PAN CFs with just 12 wt% CB exhibit a precipitous decline in strength to ~0.1 GPa (refs. 13,14). Consequently, the field lacks a synergistic processing technology capable of integrating high filler loadings without compromising structural integrity.

In this study, we present an electrified CF upgrading (ECU) strategy to engineer low-cost, low-carbon-footprint CFs by leveraging methane-derived carbon—both as pre-incorporated CB and as pyrolytic carbon deposited during synthesis. Our ECU-processed CFs, with 50 wt% CH_4-derived content, achieve a tensile strength of up to 1.7 GPa, a modulus of up to 173 GPa and an electrical conductivity of 8.5×10^4 S m^{-1}. Integrated cost and life-cycle analyses reveal that these fibres slash production costs to US$13.52 kg_{CF}^{-1} and reduce the carbon footprint to 22.39 kg_{CO2} kg_{CF}^{-1} relative to conventional PAN-based benchmarks. Beyond fibre synthesis, the ECU process facilitates the rapid fabrication of carbon/carbon (C/C) composites, dramatically condensing processing timelines while enhancing mechanical performance over traditional chemical vapour deposition (CVD). Ultimately, the ECU technique provides a scalable, industrially viable pathway for high-volume applications such as automotive manufacturing, while simultaneously mitigating climate change by sequestering potent greenhouse gas into high-value structural materials.

Results

ECU concept and design of CB/PAN CFs

Figure 1a schematically illustrates the ECU process, in which porous CFs serve as the Joule-heating element in CH_4. This process promotes CH_4 pyrolysis, resulting in carbon deposition that densifies the porous CFs, thereby enabling the simultaneous production of high-value CFs and hydrogen. We designed and synthesized CB/PAN CFs through dry-jet wet spinning of a CB/PAN composite precursor, followed by furnace heating, producing a porous microstructure composed of aligned fibril networks (Fig. 1b). These porous fibres are then used as the Joule-heating element in CH_4. The porous microstructure facilitates CH_4 diffusion throughout the material, while the Joule-heating process generates high temperatures (~1,700 K) that promote carbon deposition from CH_4 pyrolysis, as well as structural densification and refinement, leading to improved mechanical and electrical properties of the CB/PAN CFs.

Preparation of CB/PAN CFs

To fabricate a porous CB/PAN CF starting material for the ECU process, we first mixed CB (produced by conventional CH_4 pyrolysis, Fig. 2a) with PAN at various ratios (x-CB)/(100 wt% − x)-PAN, where x = 20 wt%, 30 wt%, 40 wt%, 60 wt% and 70 wt%) as the precursor for dry-jet wet spinning (Supplementary Fig. 1). The CB/PAN solutions were optimized (especially for CB particle size) to achieve uniform dispersion and a suitable viscosity for continuous spinning (Methods and Supplementary Tables 1 and 2). Using larger CB particles (for example, ~280 nm) facilitated optimal solution homogeneity and spinnability, permitting the production of CB/PAN precursor fibres with a record-high CB content of up to 70 wt%. The obtained fibre-forming solutions (Fig. 2b) were extruded through the spinneret into an air gap, followed by a coagulation bath and then drawing in a hot glycerol bath to form the precursor fibres (Fig. 2c,d). The resulting CB/PAN precursor fibres feature a unique structure composed of aligned PAN fibrils with embedded CB particles (Fig. 2e(i)). We then applied furnace heating under tension at 530 K for 20 min in air to stabilize the fibres, followed by 10 min of carbonization at 1,588 K in nitrogen. Note that the CB/PAN precursor fibres with a porous structure require less stabilization heating time (20 min; Supplementary Fig. 2) compared with pure PAN-based fibres, which typically require 1–24 h at temperatures between 473 K and 573 K (refs. 15,16), thus markedly decreasing energy consumption. After furnace heating, the PAN was successfully converted to carbon (Supplementary Fig. 3).

Figure 2f,g shows the surface and cross-sectional morphologies of the 60-CB/40-PAN CFs, showing a porous structure composed of a network of aligned carbon fibrils embedded with CB. This structure is also observed for fibres produced with different CB contents (Supplementary Fig. 4). In general, we found that lower CB loading led to smaller fibre diameters and lower pore fractions. For example, the 60-CB/40-PAN CF shows a diameter of 23.9 ± 1.1 μm and a pore fraction of 27.9% ± 1.0%, whereas the 20-CB/80-PAN CF exhibits a diameter of 12.1 ± 0.6 μm and a pore fraction of 17.8% ± 1.4% (Supplementary Fig. 5). These CB/PAN CFs remain sufficiently flexible for continuous processing and handling (Supplementary Fig. 6), while exhibiting notably enhanced mechanical properties (for example, the 20-CB/80-PAN sample features a tensile strength of ~0.8 GPa) compared with other CB-containing PAN CFs reported in the literature (for example, 12 wt% CB, ~0.1 GPa)[14]. Importantly, the fibre synthesis process achieves aligned PAN fibrils with a small diameter (for example, ~300 nm; Fig. 2e(ii),(iii)), which is attributed to the viscous effect causing the PAN solution to locally separate from the CB particles, as well as the shear-force-induced alignment of the PAN fibrils during spinning and drawing. Fibrillar morphology, typical of polymeric fibres, including PAN-based CFs[17,18], is evident in our sample (Fig. 2e). This observation is facilitated via the fibrillar separation induced by CB particles. Such a network of aligned carbon fibrils with a porous structure (Fig. 2f,g) enables CH_4 diffusion throughout the material during the ECU process and provides a strong structural scaffold to bridge the existing and newly deposited carbon species.

Synthesis and characterization of upgraded CB/PAN CFs

To conduct the ECU process, in a typical experiment, we attached the 60-CB/40-PAN CFs to two electrodes and applied a current to achieve Joule heating (Supplementary Fig. 7a–c). Different temperatures can be achieved by adjusting the magnitude of the current (Fig. 3a), which allows us to tailor the reaction. Specifically, we used a three-step Joule-heating process to upgrade the CB/PAN CFs (Fig. 3b and Supplementary Fig. 8). In step 1, we applied a current to generate a temperature of ~2,100 K for 2 min in argon to induce structural refinement of the PAN-derived carbon within the fibres (Supplementary Figs. 9 and 10). Then, in step 2, we decreased the CB/PAN CF temperature to ~1,700 K for 10 min in CH_4 to conduct the pyrolysis reaction. In addition to producing hydrogen (H_2) during this step (Methods), as the heating time increased, we found the pores in the fibres were gradually filled by the CH_4-deposited carbon, eventually forming a dense microstructure (Fig. 3c). In comparison, a low depositing temperature of 1,300 K was not enough to promote the complete pyrolysis of CH_4 to fill the pores after the 10-min treatment as a result of the slow reaction kinetics (Supplementary Fig. 11). Meanwhile, a higher pyrolysis temperature of 2,100 K led to unfilled pores and a thick carbon shell surrounding the fibres after 10 min, probably caused by the rapid carbon deposition on the surface which hinders the CH_4 diffusion to the fibre interior. Thus, a moderate heating time (for example, 10 min at 1,700 K) is necessary to fill the pores within the fibres and deposit a thin carbon layer on the fibre surface. These results demonstrate the importance of determining an appropriate pyrolysis reaction temperature and time to optimize the upgraded CB/PAN CFs. Finally, in step 3, we applied the same heating profile as used in step 1 (~2,100 K for 2 min) to promote structural refinement of the newly CH_4-deposited carbon (Supplementary Fig. 12) to produce high-performance CFs.

The surface and cross-sectional morphologies and structural analysis of the upgraded 60-CB/40-PAN CFs after the three-step ECU process reveal a dense microstructure with substantially reduced pores (Fig. 3d–f) and successful structural refinement

https://doi.org/10.1038/s41893-026-01815-w

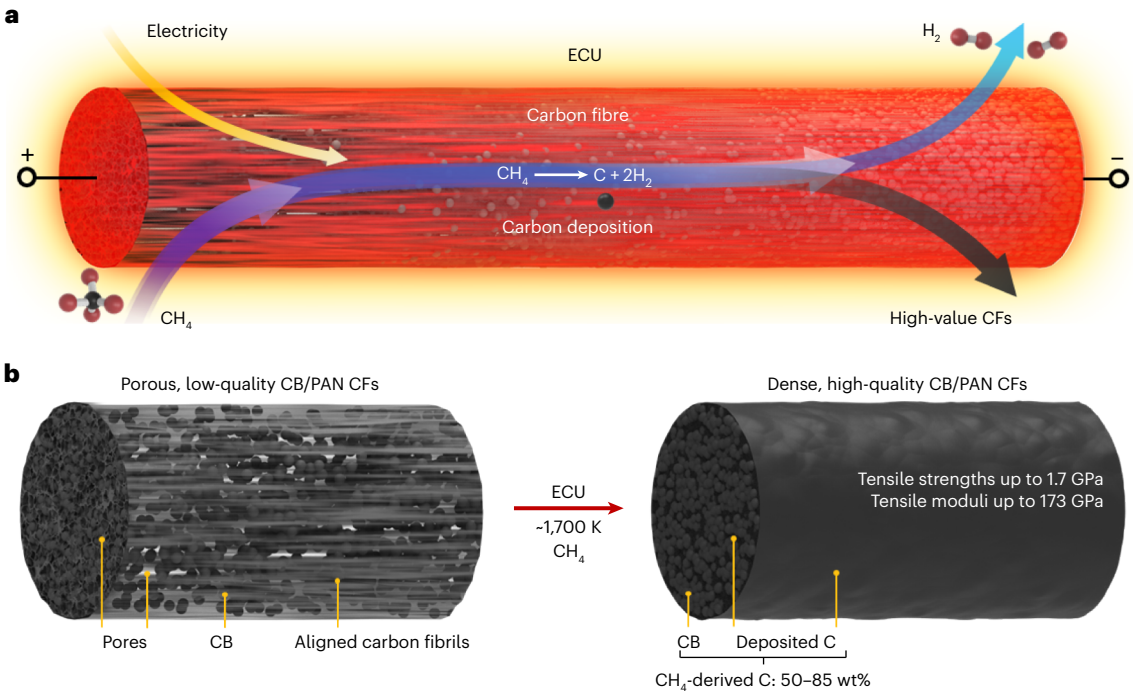

Fig. 1 | ECU by methane pyrolysis. a, Schematic of the ECU process conducted through high-temperature Joule heating with porous CFs as the Joule-heating element. The process improves the quality of the CFs by depositing carbon inside the pores. **b**, As a proof-of-concept demonstration, porous CB/PAN CFs composed of aligned fibrils embedded with CB were used as the Joule-heating substrate. In the ECU process, the resulting high temperature (~1,700 K) can pyrolyse CH_4 to produce a carbon product that fills the pores. The upgraded CB/PAN CFs feature a high content (50–85 wt%) of CH_4-derived carbon (including CB and CH_4-deposited carbon) and achieve high tensile strengths (up to 1.7 GPa) and high tensile moduli (up to 173 GPa).

(Supplementary Fig. 13a,b)[19]. For example, the pore fraction of the 60-CB/40-PAN CFs decreased from 27.9% ± 1.0% to 6.1% ± 0.8% after upgrading (Supplementary Figs. 5b and 13c,d). High-resolution transmission electron microscopy (HRTEM) imaging (Fig. 3g,h) and electron energy loss spectroscopy (EELS) analysis (Fig. 3i) of the surface and core show that the upgraded 60-CB/40-PAN CFs contain sp^2-rich carbon[20,21]. Similar morphologies were obtained when we upgraded the other CB/PAN CF samples (Supplementary Fig. 14). The porous structure of the CB/PAN CF starting material promotes CH_4 diffusion and its pyrolysis inside the pores, filling them with carbon in addition to depositing it on the fibre surface.

Properties of upgraded CB/PAN CFs

The densified microstructure of the upgraded CB/PAN CFs results in enhanced electrical and mechanical properties compared with the CB/PAN CFs before upgrading. For example, among all the CB/PAN CFs studied (Supplementary Table 3), the upgraded 60-CB/40-PAN CF exhibited the largest improvement in electrical conductivity, which increased by ~125-fold, from ~6.4×10^2 S m^{-1} (before upgrading) to ~8.0×10^4 S m^{-1} (after upgrading) (Fig. 4a and Supplementary Fig. 15a). All the upgraded CB/PAN CFs show high electrical conductivity, which is comparable to commercial CFs (for example, T300 and T700G, Fig. 4b). In addition to the electrical properties, the upgraded 60-CB/40-PAN CF showed the largest improvement in tensile strength (~8-fold), from 61 ± 21 MPa (before upgrading) to 479 ± 106 MPa (after the ECU process; Fig. 4c and Supplementary Fig. 15b). Meanwhile, the upgraded 20-CB/80-PAN CF (with tension applied during ECU) showed a tensile strength of up to 1.7 GPa (average 1.45 ± 0.25 GPa) and a modulus of up to 173 GPa (average 147 ± 28 GPa; Fig. 4d and Supplementary Fig. 16).

Overall, we attribute the high electrical and mechanical properties of the upgraded CB/PAN CFs to the dense and integrated structure achieved from carbon deposition and structural refinement within the fibre via ECU, which provides enhanced bonding between PAN- and CH_4-derived carbon. While the upgraded mechanical performance of CB/PAN CF is not intended to compete with high-end commercial CFs (Supplementary Table 4), it offers reductions in both cost and environmental impact (discussed further below), creating substantial market opportunities such as non-luxury automobiles. When compared with other low-cost CFs reported[13,22–24], our upgraded CB/PAN CFs exhibit enhanced mechanical properties (Fig. 4e and Supplementary Table 5), which closely align with the DOE requirements for low-cost CFs[7].

Economic and environmental impact of upgraded CB/PAN CFs

The upgraded CB/PAN CFs also offer cost and environmental advantages compared with pure PAN-based CFs due to the incorporation of inexpensive CH_4-derived carbon (that is, CB and CH_4-deposited carbon; Supplementary Table 6) and the electrified Joule-heating process, which has been explored in CF processing such as PAN-carbon nanotube and graphene fibres[25–31]. Using our approach, the CH_4-derived carbon can make up to 50–85 wt% of the total fibre weight (Supplementary Figs. 17 and 18). We performed a preliminary cost analysis of the upgraded 20-CB/80-PAN CFs (containing ~24 wt% CB, ~27 wt% deposited carbon and ~49 wt% PAN-derived carbon; Fig. 4f) based on the costs of the raw materials, chemicals, utilities and so on, estimating the production cost to be ~US$13.52 kg_{CF}^{-1} (Methods, Supplementary Fig. 19 and Supplementary Tables 7 and 8). This cost is lower than that of commercial high-strength CFs (for example, ~US$25.00 kg_{CF}^{-1} for T300; Supplementary Table 4) and reported low-cost CFs with comparable properties (for example, US$11.00–15.00 kg_{CF}^{-1} set by the US DOE and US$17.30 kg_{CF}^{-1} based on Oak Ridge National Laboratory production line[32]; Fig. 4g).

In addition to the cost advantage, the use of CH_4-derived carbon and reduced energy consumption during thermal treatment also reduces environmental impacts compared with pure PAN-based CFs. We conducted a simplified cradle-to-gate life-cycle assessment (LCA) for our upgraded 20-CB/80-PAN CFs, based on material inputs,

https://doi.org/10.1038/s41893-026-01815-w

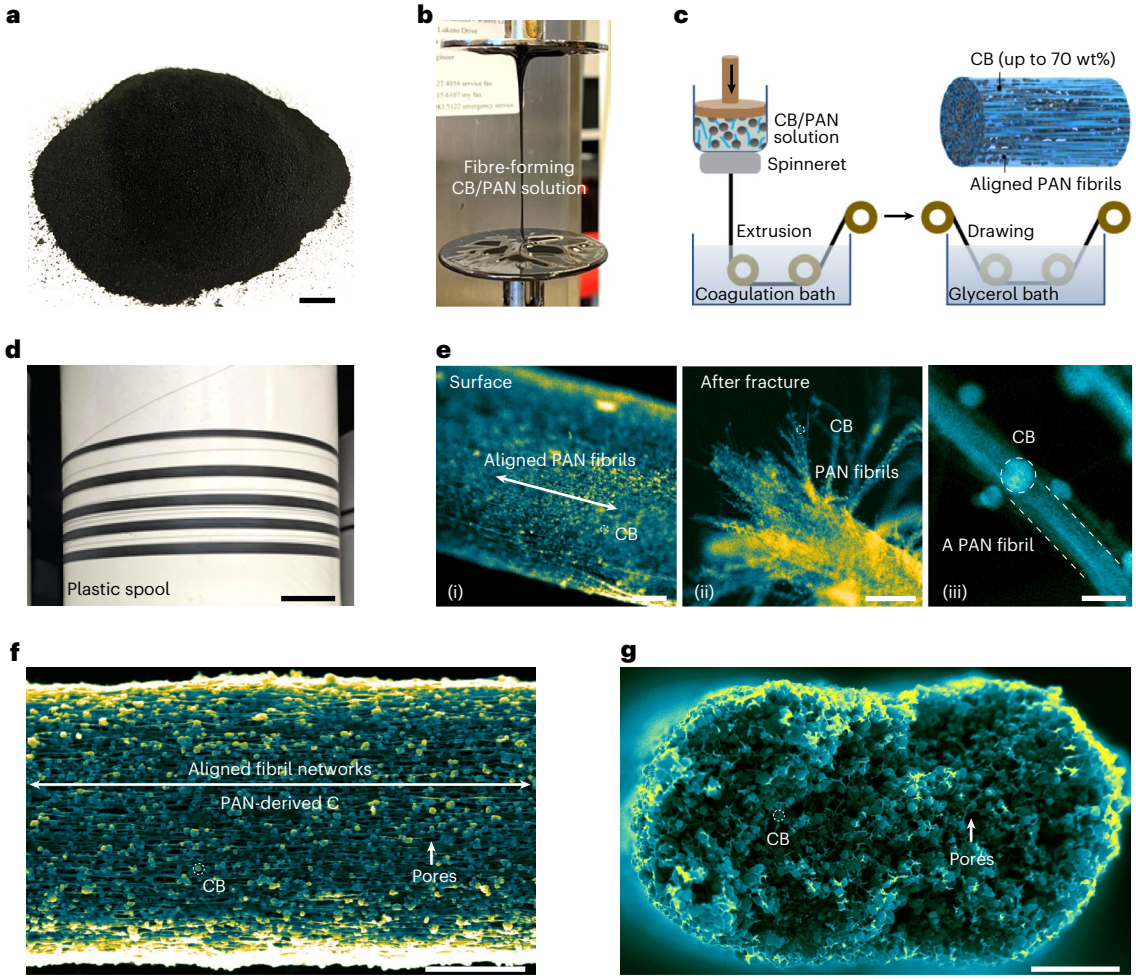

Fig. 2 | Preparation of CB/PAN CFs for the ECU process. a, Digital photo of the CB produced by conventional CH_4 pyrolysis. **b**, Digital photo of the fibre-forming CB/PAN solution. **c**, Schematic of the dry-jet wet spinning of the continuous CB/PAN precursor fibres. The inset shows a schematic of the CB/PAN precursor fibre. **d**, Digital photo of the continuous CB/PAN precursor fibres on a plastic spool. **e**, SEM (i) and scanning transmission electron microscopy (STEM, (ii) and (iii)) images of the 60-CB/40-PAN precursor fibres composed of aligned PAN fibrils and embedded CB. **f**,**g**, SEM images of the surface (**f**) and cross-sectional (**g**) morphologies of a 60-CB/40-PAN CF, showing a porous structure featuring aligned PAN-derived carbon fibrils with embedded CB particles. Scale bars: 1 cm (**a**), 2 cm (**d**), 5 µm (**e**(i)), 10 µm (**e**(ii)), 500 nm (**e**(iii)), 10 µm (**f**) and 5 µm (**g**).

outputs and process energy use (Methods). The global warming impact, reported as kilogram of CO_2 emissions per kilogram of final product CF, was calculated. The upgraded 20-CB/80-PAN CFs exhibited a lower CO_2 emission value of ~22.39 kg_{CO2} kg_{CF}^{-1} (Supplementary Table 9), compared with ~30.00 kg_{CO2} kg_{CF}^{-1} for pure PAN-based CFs[33]. A key contributor to this reduction is the decreased CO_2 output associated with both the production of carbon feedstocks and carbon loss during fibre processing. Specifically, the CO_2 emissions for pure PAN-based CFs are ~12.64 kg_{CO2} kg_{CF}^{-1}, whereas for lignin-derived CFs, the output is ~9.01 kg_{CO2} kg_{CF}^{-1}. Meanwhile, the CO_2 output for our CB/PAN CFs is only ~7.23 kg_{CO2} kg_{CF}^{-1} (Fig. 4h and Supplementary Table 10), underscoring the environmental advantage of incorporating CH_4-derived carbon as a partial PAN substitute.

Besides the cost and environmental benefits, the ECU process presents a promising approach for the continuous upgrading of low-quality CFs (Fig. 4i and Supplementary Fig. 20). We have designed and implemented a roll-to-roll system in which aligned CFs are unwound from a supply spool and fed between two conductive graphite rods which serve as electrodes for Joule heating the fibres while maintaining fibre tension. An electric current flows through the segment of CFs between the electrodes, driving the resistive heating process. Under the flow of CH_4, the CFs become densified as the pyrolysis reaction proceeds. The densified CFs are subsequently heated in an inert atmosphere to refine the microstructure and thus produce high-quality CFs. The proposed ECU system can be integrated into existing fibre manufacturing setups with minimal modifications (Supplementary Fig. 21).

Fabrication of C/C composites via ECU

Beyond its capability to densify individual CFs, our ECU process, distinguished by the in situ high-temperature decomposition of CH_4 into carbon, can also be used to conformally bond CFs together (Fig. 5a) to create CF-reinforced C/C composites (one of the most widely applied forms of CF products)[34], thus offering improved process intensification. As a proof-of-concept demonstration, we used the upgraded 20-CB/80-PAN CFs to fabricate C/Cs via ECU (Methods and Supplementary Fig. 22). Our CB/PAN CF-based C/C had a tensile strength of 0.40 ± 0.06 GPa (Fig. 5b) and a dense structure (Fig. 5c), which is comparable to the strength (~0.38 GPa) of reported C/Cs (comprised of commercial T300 CFs and CH_4-deposited carbon) that were prepared at 1,373 K over a 10-h duration under 20 kPa using conventional CVD[35,36]. Additionally, we used T300 CFs to prepare the C/C via ECU (Methods). Choosing T300 CFs enabled us to directly compare the C/Cs produced using the ECU and conventional methods, all based on the same material platform but using different techniques. Our T300

https://doi.org/10.1038/s41893-026-01815-w

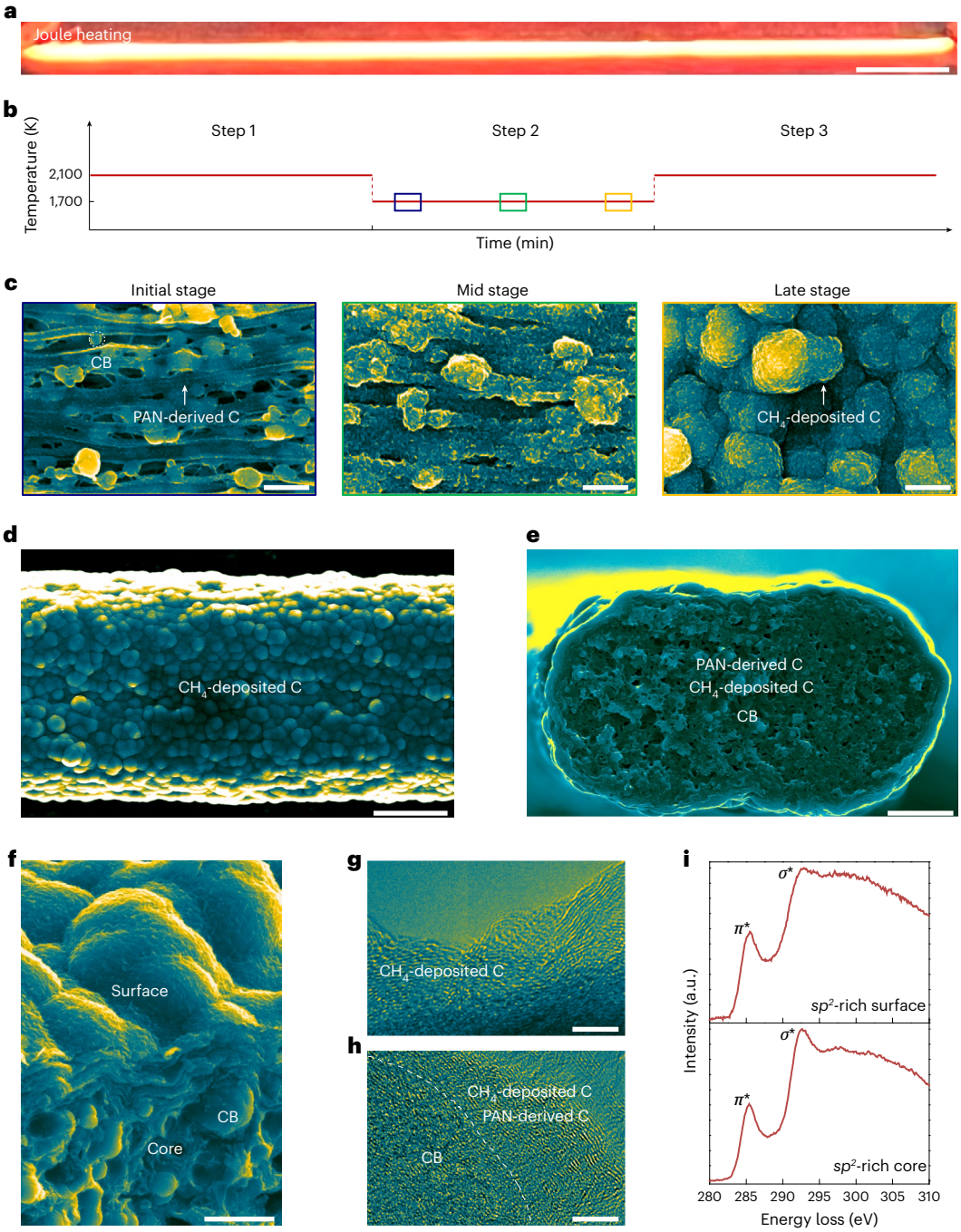

Fig. 3 | The ECU process and the microstructure of the upgraded CB/PAN CFs. **a**, Digital photo of the CB/PAN CFs during Joule heating, which is used to modify the fibre microstructure via the ECU process. **b**, Schematic of the three-step upgrading process: step 1, structural refinement of the PAN-derived carbon in argon at 2,100 K for 2 min; step 2, CH_4 pyrolysis in CH_4 at 1,700 K for 2–10 min (depending on various fibres) to deposit carbon in the fibre pores; and step 3, structural refinement of the CH_4-deposited carbon in argon at 2,100 K for 2 min. **c**, SEM images of the surface morphology of a 60-CB/40-PAN CF at different heating times during step 2 (initial, mid and late stages of carbon deposition). **d**–**f**, SEM images of the surface (**d**) and cross-sectional (**e**,**f**) morphologies of the upgraded 60-CB/40-PAN CF, showing a dense structure. **g**,**h**, HRTEM images of the surface (**g**) and core (**h**) structure of the upgraded 60-CB/40-PAN CF. **i**, EELS analysis of the upgraded 60-CB/40-PAN CF, including the surface (**g**) and core (**h**) of the fibre. The high intensity of σ^* indicates the presence of rich sp^2 carbon compared with amorphous carbon[20]. Scale bars, 0.5 cm (**a**), 1 μm (**c**), 10 μm (**d**), 5 μm (**e**), 1 μm (**f**), 5 nm (**g**) and 5 nm (**h**).

CF-based C/C also showed a high tensile strength of 0.68 ± 0.07 GPa (Fig. 5b) and a dense structure (Fig. 5d). This strength substantially exceeds that of previously reported CF-based C/Cs (~0.38GPa for C/Cs without binders and ~0.50–0.65 GPa for C/Cs with the addition of costly carbon nanotube binders)[35,36]. Importantly, our process only takes ~40 min, which is considerably shorter than conventional methods such as CVD (>10 h; Fig. 5e).

Our ECU provides uniform in situ heating, avoiding thermal gradients in the C/C and promoting effective CH_4 pyrolysis for uniform carbon deposition throughout the composite. Simultaneously, the applied tension keeps the fibres aligned during heating, contributing to better mechanical performance of the C/C. Therefore, our ECU method presents a pioneering platform to leverage CH_4-derived carbon for the synthesis of not only CFs but also C/Cs.

https://doi.org/10.1038/s41893-026-01815-w

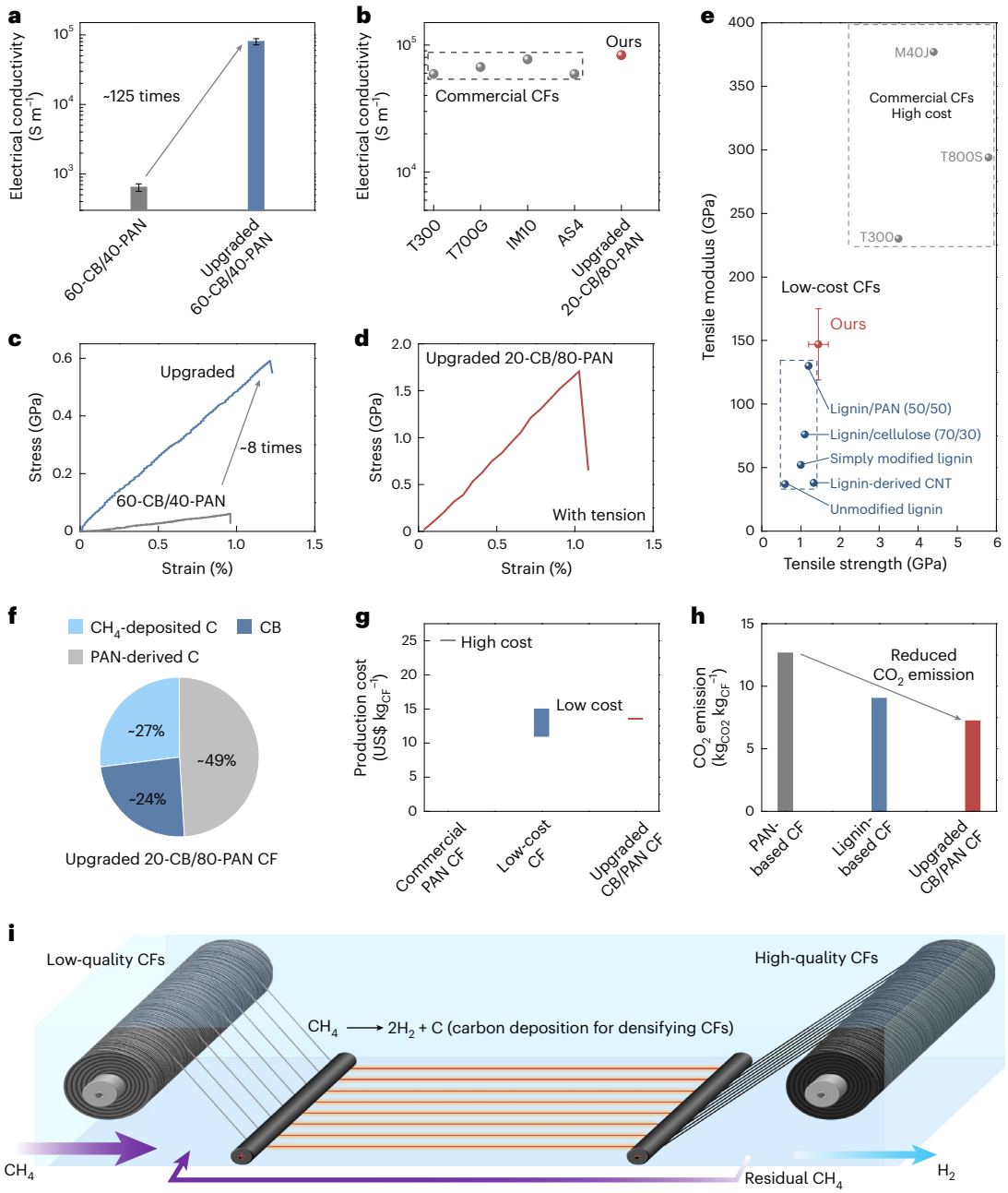

Fig. 4 | Performance of the upgraded CB/PAN CFs and schematic of the scalable ECU process for producing upgraded CFs. a, The electrical conductivity of the 60-CB/40-PAN and upgraded 60-CB/40-PAN CFs, showing ~125-fold improvement. Data from eight independent measurements ($n = 8$) are presented as mean ± s.d. Bar heights represent mean values and error bars indicate standard deviation. **b**, The electrical conductivity of the upgraded CB/PAN CFs compared with various commercial CFs (for example, T300 and T700G). **c**, The stress–strain curves of the 60-CB/40-PAN and upgraded 60-CB/40-PAN CFs. The tensile strength of the upgraded fibre increased by about eight times compared with the fibre before upgrading. **d**, The stress–strain curve of the upgraded 20-CB/80-PAN CFs (with tension applied during the ECU process), showing the highest tensile strength of up to 1.7 GPa and modulus of up to 173 GPa. **e**, Mechanical property comparison of our upgraded 20-CB/80-PAN CFs with high-cost commercial CFs and other reported low-cost CFs. Data from eight independent measurements ($n = 8$) are presented as mean ± s.d. Red circle markers represent mean values and error bars indicate standard deviation. Other circle markers denote data from the literature[13,22–24]. **f**, Content of PAN- and CH_4-derived carbon (CB- and CH_4-deposited carbon) in the upgraded 20-CB/80-PAN CFs. **g**, Comparison of the production costs of conventional PAN CFs (for example, T300), low-cost CFs defined by US DOE and our upgraded 20-CB/80-PAN CFs. **h**, CO_2 emissions associated with both the production of carbon feedstocks and carbon loss during fibre processing for pure PAN-based, lignin-based and our upgraded 20-CB/80-PAN CFs. **i**, Proposed scheme of the scaled ECU process for the production of high-quality CFs using low-quality CFs as the Joule-heating elements.

Discussion

Traditional methane pyrolysis typically yields low-value CB, a factor that fundamentally constrains its economic viability and long-term sustainability. While catalytic methods have been proposed to synthesize higher-order architectures, such as carbon nanotubes, they are often hampered by energy-intensive catalyst recovery and complex downstream purification. In contrast, our ECU strategy offers a catalyst-free, electrified pathway that directly transforms CH_4 into high-value structural CFs while simultaneously cogenerating green hydrogen. Although the absolute mechanical metrics of CH_4-derived

https://doi.org/10.1038/s41893-026-01815-w

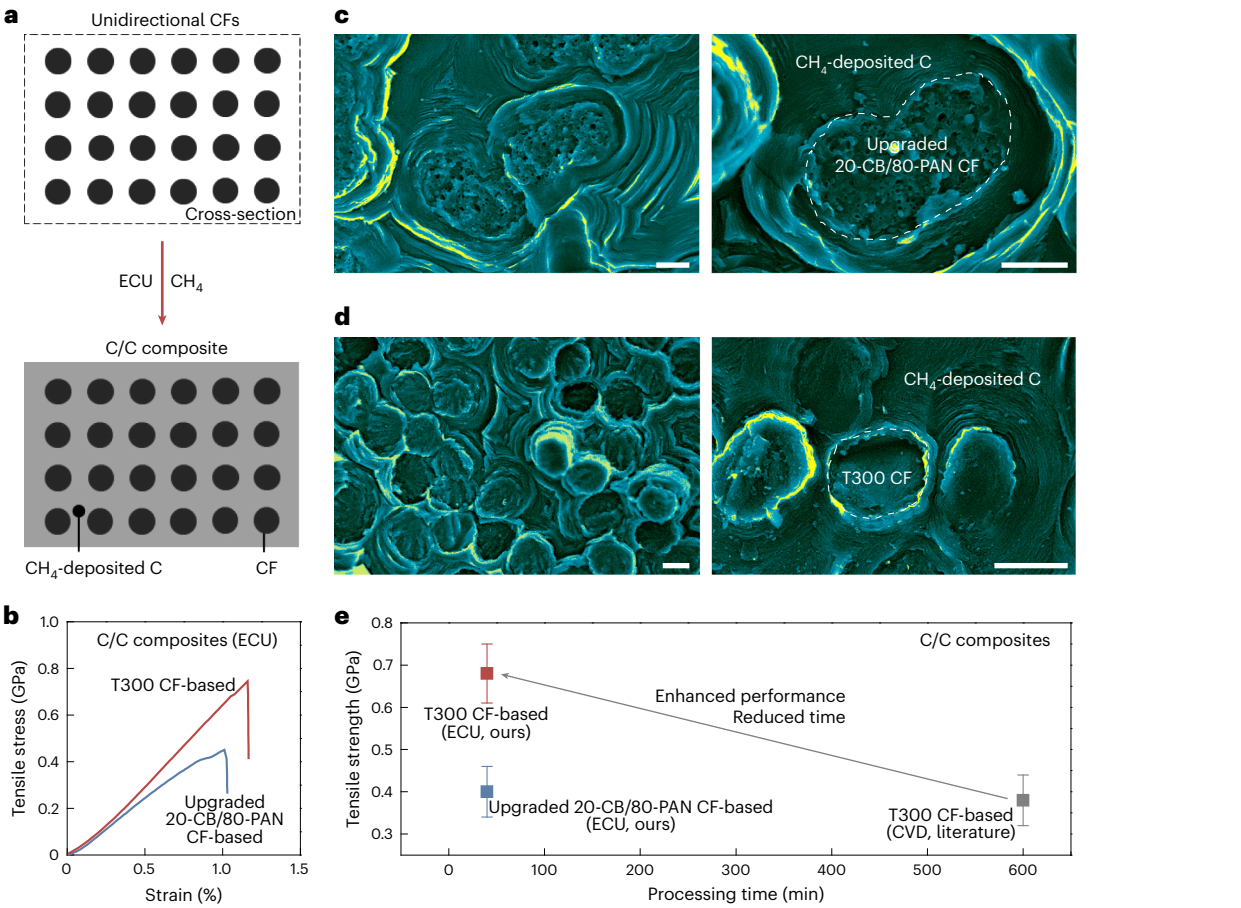

Fig. 5 | CF-reinforced C/C composites fabricated using our ECU method. **a**, Schematic of the preparation of CF-reinforced C/Cs by ECU. **b**, The stress–strain curves of the upgraded 20-CB/80-PAN CF-based C/Cs and T300 CF-based C/Cs, prepared using our ECU. **c**,**d**, SEM images of cross-sectional morphologies of the upgraded 20-CB/80-PAN CF-based C/Cs (**c**) and T300 CF-based C/Cs (**d**), synthesized using our ECU. **e**, Comparison of the tensile strength and processing time for the C/Cs using our ECU and traditional CVD methods. Data from five independent measurements ($n = 5$) are presented as mean ± s.d. Square markers represent mean values and error bars indicate standard deviation. The grey square marker denotes data from the literature[35,36]. Scale bars: 5 µm (**c**) and 5 µm (**d**).

CFs currently trail those of premium PAN-based benchmarks, their drastically reduced production cost and life-cycle carbon footprint present a transformative value proposition. These attributes render such fibres uniquely suited for high-volume, price-sensitive industries—most notably mass-market automotive manufacturing—where the coproduced H_2 could serve as a decentralized energy supply, further enhancing the systemic efficiency of the ECU process.

When powered by renewable electricity and fed by biomethane, the ECU platform could achieve a carbon-negative potential by sequestering CH_4 into solid-state carbon without direct emissions. Beyond remediating low-grade precursors (such as biomass- or CB-based fibres), this approach provides a universal template for converting abundant feedstocks into a diverse class of value-added materials, including high-performance C/C composites. Ultimately, the ECU framework demonstrates that integrating advanced materials synthesis with clean energy coproduction can forge a sustainable nexus between industrial manufacturing and global climate change mitigation.

Methods

Materials

Poly(acrylonitrile-co-methacrylic acid) (PAN, 4 wt% copolymers) with a molecular weight of 500,000 g mol^{-1} was used as the polymer binder and obtained from Japan Exlan. Dimethylformamide (DMF, ACS grade, 99.8%) was obtained from Sigma-Aldrich. Thermal CB (CB, Commercial Thermax N991; produced by the thermal decomposition of high-purity methane feedstock) with a diameter of 200–400 nm was purchased from Cancarb. Methane (ultrahigh-purity grade, ME UHP300) and argon (ultrahigh-purity grade, AR UHP300) were purchased from Airgas.

Preparation of CB/PAN solutions

To prepare the CB/PAN solutions with different CB sizes/contents, the CB was first dispersed in DMF via 24h of sonication at a concentration determined by the target solid content. The CB/PAN solutions were then prepared by mixing dried PAN with the chilled (273 K) CB/DMF solution for 1 h, followed by increasing the temperature to 343 K and further stirring. After 2 h, the fibre formability of the solution was checked by observing whether thin fibres could be produced when a glass rod was withdrawn from the solution. The complex viscosity was measured using a parallel-plate rheometer to confirm that the solution had an appropriate viscosity for spinning. On the basis of the assessed fibre-forming behaviour and measured viscosity, DMF was added or evaporated while mixing until fibre formation was observed and the complex viscosity was within an acceptable range for fibre spinning (Supplementary Tables 1 and 2).

Spinning of CB/PAN precursor fibres

Dry-jet wet spinning was conducted on a single-filament system designed by Hills, in which the CB/PAN solutions were extruded through a spinneret (for example, 200 µm) into an air gap of 3 cm to 5 cm, followed by a coagulation bath of methanol (MeOH) and dimethyl acetamide (DMAc, 70/30 v/v). The fibres were drawn by passing the

fibre through a glycerol bath at ~438 K. The resulting CB/PAN filaments were wound onto a spool. To prepare the CB/PAN precursor fibres for heat treatment, these filaments were removed from their spools in bundles resembling fibre tows.

Stabilization and carbonization of CB/PAN precursor fibres

Stabilization of the CB/PAN precursor fibres was performed in a tube furnace (MHI H17HT2.5×24, Micropyretics Heaters International), consisting of a 20-min isothermal hold at 530 K with a supplied air atmosphere. Carbonization was then performed in a tube furnace by heating the fibre bundle in a nitrogen atmosphere from room temperature to 1,588 K at a rate of 5 K min^{-1}. The fibres were kept at 1,588 K for 10 min and then cooled down to room temperature at a 5 K min^{-1} ramp-down rate. During stabilization and carbonization, a stress (5 MPa for 70-CB/30-PAN, 60-CB/40-PAN and 40-CB/60-PAN and 15 MPa for 30-CB/70-PAN and 20-CB/80-PAN) was applied using graphite and stainless-steel weights, as tension during stabilization and carbonization has been shown to improve the mechanical properties of the fibres[37]. After carbonization, these bundles were used in the ECU process.

Joule heating of CB/PAN CFs

The Joule-heating system without hanging weights (batch upgrading without tension; Supplementary Fig. 7a–c) includes calibrated mass flow controllers, a microflow quartz tube reactor (inner diameter of 1.27 cm, length of 20.32 cm, reactor volume of 25.73 cm^3, Omega) and an external power source (Keithley 2425, Tektronix; or HY6020EX-60A, VOL TEQ). Both ends of the quartz tube were attached to Ultra-Torr tee fittings (Swagelok), where one port of each tee was used to accommodate the electric wires, while the other was used as a gas inlet/outlet. A bundle of CB/PAN CFs was attached to the copper electrodes supported by a homemade alumina ceramic holder. The holder was placed in the quartz tube, with both ends of the holder connected to a power source by copper wires (8873K15, McMaster Carr) that fed through the alumina ceramic tubes (single hole, ORX-11618, Omega). Joule heating was performed under ambient pressure by varying the current and its duration applied to the CFs using the connected power source to achieve different heating temperatures. A three-step heating process was used as follows. In step 1, we applied a constant current to generate a high temperature of ~2,100 K for 2 min to induce structural refinement of the fibres in argon. In step 2, we first applied an initial current and gradually increased the current at a rate of 0.1–1.0 A min^{-1} to generate a temperature of ~1,700 K for different heating times (10 min for 70-CB/30-PAN and 60-CB/40-PAN, 5 min for 40-CB/60-PAN and 30-CB/70-PAN and 2 min for 20-CB/80-PAN) to upgrade the fibres in CH_4. Step 2 results in a decrease in the resistance of the upgraded CB/PAN CFs with the heating time due to fibre densification, which makes it necessary to increase the applied current to maintain the fibres at a constant high temperature. In step 3, we applied a constant current to generate a high temperature of ~2,100 K for 2 min to induce structural refinement of the fibres in argon.

The Joule-heating system with hanging weights (batch upgrading with tension; Supplementary Fig. 7d–f) contains calibrated mass flow controllers, a quartz tube reactor (inner diameter of 5.5 cm, length of 60.0 cm, reactor volume of 330.0 cm^3, Omega) and an external power source. In a typical process, the CF ends were fixed between graphite/stainless-steel weights, then attached to graphite rods, which were suspended on a specially designed ceramic tray. This arrangement was placed within a quartz tube and connected to a power source. Considering the improvement of the mechanical performance of the fibres, we used the setup with tension to upgrade the 20-CB/80-PAN CFs (applying a stress of 2 MPa).

Preparation of C/C composites

In a typical experiment, the two ends of the upgraded 20-CB/80-PAN CFs (an ~5-cm long bundle containing ~500 filaments) were secured between graphite/stainless-steel sheets. The fibres were then subjected to a stress (3 MPa), induced by graphite and stainless-steel weights and placed on a customized ceramic tray. The initial upgrading of the bundle was carried out in CH_4 at ~1,700 K for 35 min under ambient pressure, followed by structural refinement of the C/C in argon at ~2,100 K for 5 min. The spaces between the CFs within the bundle were filled by the CH_4-deposited carbon. We also used 1,000 T300 CFs (an ~5-cm long bundle) to prepare the C/C via our ECU method. This process mirrored the fabrication of the CB/PAN CF-based C/Cs. Before use, the T300 CFs were de-sized with acetone for 6 h and rinsed with deionized water.

Mechanical measurement and calculation

Tensile testing was performed on an RSA Solids Analyzer II and an Instron 5943, using a gauge length of 0.635 cm for CFs before and after upgrading, as well as for C/Cs. A single filament (for CFs) or bundle (for C/Cs) was mounted on a paper frame using thermoset epoxy. To conduct the tensile test, the ends of the paper frame were clamped in the machine, then the paper frame was cut and a linear strain was applied. ImageJ was used to measure the diameter, cross-sectional area and pore area in SEM images of the fibre cross-sections. The tensile properties of the fibres/composites were calculated from the obtained stress–strain curves according to the diameter (or the overall cross-sectional area). The contents of PAN-derived carbon, CB and CH_4-deposited carbon in the upgraded CB/PAN CFs were evaluated by their geometrical sizes in the cross-section (Supplementary Fig. 17).

Electrical conductivity measurement and calculation

The electrical conductivity of CB/PAN CFs before and after upgrading was determined using a two-probe resistance measurement technique (Keithley 2400/2425, Tektronix). Single-filament fibres were secured to a piece of glass with colloidal silver paste, which served as contacts for the probes. The length and diameter of the fibre between the probes were measured using ImageJ software. The resistance was then determined by measuring the potential between the probes over a sweep of applied currents from 0.5 μA to 500 μA and the conductivity was evaluated on the basis of the fibre geometry. The electrical conductivity of commercial CFs can be found on the manufacturers' websites, including the datasheets for Toray T300 and T700G (https://www.toraycma.com/resources/data-sheets) and for Hexcel IM10 and AS4 (https://www.hexcel.com/products/carbon-fiber).

Materials characterization

Wide-angle X-ray diffraction of the fibre bundles was conducted on a Rigaku MicroMax-003 coupled to an R-axis IV++ detector. Rheological properties of the CB/PAN solutions were measured on an ARES rheometer using parallel-plate geometry (25 mm in diameter and 1 mm gap). Thermogravimetric analysis (TGA, Q500, TA Instruments) was used to measure the solid content of the spinning solution. For this purpose, samples were heated to 403 K in air until a constant weight was reached. Scanning electron microscopy (SEM) images were collected using Hitachi SU8230, Hitachi 2700 C and FEI Helios microscopes. HRTEM images, electron diffraction patterns and EELS were collected using JEOL 2100 F and Hitachi 2700 C. To reduce the charging of CB/PAN precursor fibres during TEM/SEM characterization, a double-fold copper TEM grid (50/50 mesh) was sandwiched around the sample. We used a microbalance (Mettler Toledo, WXTS3DU) to determine the mass of various CB/PAN CFs and then calculated their volumes using the geometric dimensions for each sample. Knowing both the mass and volume enabled the calculation of density using the formula: density = mass/volume. The Joule-heated fibres emit light, which was recorded by a high-speed camera (Vision Research Phantom v.12.0) to determine the temperature of the material by evaluating ratios of the raw RGB channel intensities[38,39].

Measurement of CH_4 conversion and H_2 yield

Our upgrading process facilitates CH_4 pyrolysis, resulting in the production of carbon and H_2. The CH_4 conversions and H_2 yields in the

electrified CH_4 pyrolysis reaction were determined through offline analyses. The ECU process in step 2 generates H_2 with a yield of 85.4% ± 4.3% (at a CH_4 conversion of 93.2% ± 2.5%). We used a mixture of CH_4 (2.5 ml min^{-1}) and argon (0.5 ml min^{-1}, as an internal standard) to flow through the heating element in the setup (without hanging weights) during the ECU process. During upgrading, the gas products were collected at the outlet of the reactor using a multilayer foil sampling bag (0.6 l, Supel-Inert Multi-Layer Foil). The sample bag was brought to a gas chromatograph (Agilent, Model 6890 N) equipped with a thermal conductivity detector (ShinCarbon ST packed column, Restek) to quantify gas compositions. The sample was transferred from the gas sampling bag into the gas chromatograph by a gas-tight syringe (50 µl, Hamilton 1705). Equation (1) was used to calculate the CH_4 conversion (%) from the concentration difference between the feed ($n_{CH_4,feed}$) and product ($n_{CH_4,product}$) stream.

$$\text{Conversion}_{CH_4}(\%) = \frac{n_{CH_4,feed} - n_{CH_4,product}}{n_{CH_4,feed}} \times 100\,\% \quad (1)$$

The H_2 yield (%) was calculated from equation (2), where n_{H_2} is H_2 concentration in the product stream.

$$\text{Yield}_{H_2}(\%) = \frac{n_{H_2}}{2 \times n_{CH_4,feed}} \times 100\,\% \quad (2)$$

Cost analysis of the upgraded 20-CB/80-PAN CFs

We estimated the production cost of the upgraded 20-CB/80-PAN CFs to be ~US$13.52 kg_{CF}^{-1}. The major cost components, namely raw materials, chemicals, utilities and other process costs are detailed below (Supplementary Fig. 19 and Supplementary Tables 7 and 8). The techno-economic analysis (TEA) results were based on our experimental data as well as data gathered from the literature and publicly available sources.

For raw materials, the upgraded CB/PAN CF contained PAN-derived carbon (~US$6.00 kg_{PAN}^{-1}), CB (~US$1.00 kg_{CB}^{-1}) and CH_4-deposited carbon. PAN undergoes mass loss during stabilization and carbonization steps (45–50 wt%)[40], whereas CB- and CH_4-deposited carbon were assumed not to experience such loss. To produce 1 kg of final upgraded 20-CB/80-PAN CFs, the required inputs were ~0.25 kg of CB, ~0.25 kg of methane-derived carbon, produced from 0.391 kg of CH_4 in our case and ~1.00 kg of PAN. On the basis of the cost of ~US$6.00 kg_{PAN}^{-1}, the PAN precursor cost was estimated at ~US$6.00 kg_{CF}^{-1}. Similarly, the CB cost was ~US$0.25 kg_{CF}^{-1} and the CH_4 cost (at US$0.29 kg_{CH4}^{-1}) was ~US$0.11 kg_{CF}^{-1}. This resulted in a total raw materials cost of US$6.36 kg_{CF}^{-1}.

Several solvents were used in the process for specific functions. DMF was used to dissolve PAN and disperse CB to form the precursor solution; MeOH and DMAc served as a coagulation bath to solidify the precursor into fibres; and glycerol was used as a thermal medium during the hot drawing of the coagulated fibres. The estimated solvent losses were as follows: DMF at 0.14 kg (costing US$1.5 kg_{DMF}^{-1}), MeOH at 0.06 kg (US$0.5 kg_{MeOH}^{-1}), DMAc at 0.03 kg (US$1.0 kg_{DMAc}^{-1}) and glycerol at 0.13 kg (US$0.8 $kg_{glycerol}^{-1}$). These chemicals contributed to a total cost of US$0.37 kg_{CF}^{-1}.

Utilities used in the process included electricity, nitrogen gas and air. Electricity was consumed during several thermal processing stages. In the furnace process, energy was used for stabilization at 530 K in air for 20 min, consuming 43.60 MJ kg_{CF}^{-1} and carbonization at 1,588 K in nitrogen for 10 min, consuming 146.69 MJ kg_{CF}^{-1}. For the ECU upgrades specific to CB/PAN CFs, electricity was used in three steps: step 1, structural refinement at 2,100 K in nitrogen for 2 min, consuming 47.7 MJ kg_{CF}^{-1}; step 2, CH_4 pyrolysis and carbon deposition at 1,700 K in methane for 2 min, consuming 21.0 MJ kg_{CF}^{-1}; and step 3, final structural refinement at 2,100 K in nitrogen for 2 min, consuming another 47.7 MJ kg_{CF}^{-1}. The total energy consumption was therefore 306.69 MJ kg_{CF}^{-1} (equivalent to 85.19 kWh). At an electricity rate of US$0.03 kWh^{-1} (per the US DOE 2030 target), the electricity cost was estimated to be US$2.56 kg_{CF}^{-1}. Additionally, ~1.75 kg of nitrogen gas (at US$0.12 kg_{N2}^{-1}) was used during carbonization, adding US$0.21 kg_{CF}^{-1}. The total utilities cost was thus US$2.77 kg_{CF}^{-1}.

No substantial change was expected in other processing costs such as sizing, drying, winding, packaging, emissions treatment, labour, overhead, maintenance and capital depreciation. Therefore, we adopted the previously reported estimate of US$4.02 kg_{CF}^{-1} for these other costs.

LCA of the upgraded 20-CB/80-PAN CFs

The LCA was performed using the SimaPro software (https://simapro.com), which incorporates the primary US Life Cycle Inventory Database (https://www.nlr.gov/analysis/lci). In this preliminary LCA evaluation, we focused on feedstock/raw materials, chemicals and utilities (electricity and gas) consumption. Using these results, we used the TRACI method[41] to determine the environmental impacts of our upgraded 20-CB/80-PAN CFs.

The goal of this LCA was to evaluate the carbon footprint associated with the production of the upgraded 20-CB/80-PAN CFs, which used reduced PAN feedstock and lower heating energy requirements to minimize the global warming potential of the product and process. A cradle-to-gate LCA approach was adopted with a functional unit of 1 kg of upgraded 20-CB/80-PAN CFs. The system boundary included upstream impacts from feedstocks (PAN, CB and CH_4), chemicals (DMF, DMAc, MeOH and glycerol), electricity for heating processes and gas used in the production of the upgraded 20-CB/80-PAN CFs. The use phase and end-of-life treatment of the upgraded 20-CB/80-PAN CFs were excluded from this assessment.

For 1 kg of upgraded 20-CB/80-PAN CFs, the cradle-to-gate LCA yielded total CO_2-equivalent emissions of 22.39 kg_{CO2} kg_{CF}^{-1}. PAN production and volatilization contributed 6.32 kg_{CO2} kg_{CF}^{-1}. Approximately 1.0 kg of PAN was consumed, generating 5.7 kg_{CO2} during precursor synthesis. During stabilization and carbonization, 0.5 kg_{PAN} was lost, of which 0.17 kg was carbon, resulting in an additional 0.62 kg_{CO2}. The use of 0.25 kg_{CB} contributed an estimated 0.595 kg_{CO2} kg_{CF}^{-1}. Methane use required 0.391 kg CH_4, with upstream production contributing 0.137 kg_{CO2} kg_{CF}^{-1}. Oxidation of off-gas, comprising 0.027 kg CH_4 and 0.03 kg C_xH_y, added 0.18 kg kg_{CO2} kg_{CF}^{-1}. The total methane-associated emissions were 0.317 kg_{CO2} kg_{CF}^{-1}.

Solvent-related emissions amounted to 1.641 kg_{CO2} kg_{CF}^{-1}. During solvent production, DMF, MeOH, DMAc and glycerol contributed 0.293 kg_{CO2} kg_{CF}^{-1}, 0.063 kg_{CO2} kg_{CF}^{-1}, 0.077 kg_{CO2} kg_{CF}^{-1} and 0.628 kg_{CO2} kg_{CF}^{-1}, respectively.

Volatilization losses during processing contributed a further 0.26 kg_{CO2} from DMF, 0.07 kg_{CO2} from MeOH, 0.07 kg_{CO2} from DMAc and 0.18 kg_{CO2} from glycerol, for a total of 0.58 kg_{CO2} kg_{CF}^{-1}. Future work should explore safer and more sustainable solvents to reduce CO_2 emissions.

Electricity consumption was 85.19 kWh per kilogram of upgraded 20-CB/80-PAN CFs, corresponding to 12.69 kg_{CO2} kg_{CF}^{-1} under the assumed grid emission factors. In addition, production of 1.75 kg of nitrogen gas contributed 0.831 kg_{CO2} kg_{CF}^{-1}.

Reporting summary

Further information on research design is available in the Nature Portfolio Reporting Summary linked to this article.

Data availability

The data that support the findings of this study are available in this paper and its Supplementary Information. Source data are provided with this paper.

References

1. Chae, H. G. et al. High strength and high modulus carbon fibers. *Carbon* **93**, 81–87 (2015).

2. Anguita, J. V. et al. Dimensionally and environmentally ultra-stable polymer composites reinforced with carbon fibres. *Nat. Mater.* **19**, 317–322 (2020).
3. Chae, H. G. & Kumar, S. Making strong fibers. *Science* **319**, 908–909 (2008).
4. Khayyam, H. et al. PAN precursor fabrication, applications and thermal stabilization process in carbon fiber production: experimental and mathematical modelling. *Prog. Mater. Sci.* **107**, 100575 (2020).
5. Choi, D., Kil, H. & Lee, S. Fabrication of low-cost carbon fibers using economical precursors and advanced processing technologies. *Carbon* **142**, 610–649 (2019).
6. Adams, J. J. et al. *Consortium for Production of Affordable Carbon Fibers in the United States* (US Department of Energy, 2021).
7. Peijs, T., Kirschbaum, R. & Lemstra, P. J. Chapter 5: A critical review of carbon fiber and related products from an industrial perspective. *Adv. Ind. Eng. Polym. Res.* **5**, 90–106 (2022).
8. Das, S., Warren, J., West, D. & Schexnayder, S. M. *Global Carbon Fiber Composites Supply Chain Competitiveness Analysis* (US Department of Energy, 2016).
9. Xu, Y., Liu, Y., Chen, S. & Ni, Y. Current overview of carbon fiber: toward green sustainable raw materials. *BioResources* **15**, 7234–7259 (2020).
10. Islam, M. T., Howlader, M. S., Shuvo, D. M. & Uddin, M. K. Carbon fiber from biomass sources: a comprehensive review. *Non-Met. Mater. Sci.* **5**, 14–26 (2023).
11. Sun, S. C., Xu, Y., Wen, J. L., Yuan, T. Q. & Sun, R. C. Recent advances in lignin-based carbon fibers (LCFs): precursors, fabrications, properties, and applications. *Green Chem.* **24**, 5709–5738 (2022).
12. Li, J. et al. Lignin molecular design to transform green manufacturing. *Matter* **5**, 3513–3529 (2022).
13. Jin, J. & Ogale, A. A. Carbon fibers derived from wet-spinning of equi-component lignin/polyacrylonitrile blends. *J. Appl. Polym. Sci.* **135**, 45903 (2018).
14. Ahn, D., Choi, H., Kim, H. & Yeo, S. Y. Properties of conductive polyacrylonitrile fibers prepared by using benzoxazine modified carbon black. *Polymers* **12**, 179 (2020).
15. Gupta, A. & Harrison, I. R. New aspects in the oxidative stabilization of PAN-based carbon fibers: II. *Carbon* **35**, 809–818 (1997).
16. Lu, M. et al. Stabilization of polyacrylonitrile fibers with carbon nanotubes. *Polym. Degrad. Stab.* **188**, 109567 (2021).
17. Perret, R. & Ruland, W. The microstructure of PAN-base carbon fibres. *J. Appl. Crystallogr.* **3**, 525–532 (1970).
18. Diefendorf, R. J. & Tokarsky, E. High-performance carbon fibers. *Polym. Eng. Sci.* **15**, 150–159 (1975).
19. Duy, L. X. et al. Laser-induced graphene fibers. *Carbon* **126**, 472–479 (2018).
20. Ahn, C. C., Krivanek, O. L., Burgner, R. P., Disko, M. M. & Swann, P. R. *EELS Atlas: A Reference Collection of Electron Energy Loss Spectra Covering All Stable Elements* (Gatan, 1983).
21. Li, J. T. et al. Laser-induced glassy carbon nanofiber trees. *Carbon* **215**, 118494 (2023).
22. Zhang, M. & Ogale, A. A. Carbon fibers from dry-spinning of acetylated softwood kraft lignin. *Carbon* **69**, 626–629 (2014).
23. Hosseinaei, O., Harper, D. P., Bozell, J. J. & Rials, T. G. Role of physicochemical structure of organosolv hardwood and herbaceous lignins on carbon fiber performance. *ACS Sustain. Chem. Eng.* **4**, 5785–5798 (2016).
24. Bengtsson, A. et al. Carbon fibers from lignin-cellulose precursors: effect of carbonization conditions. *ACS Sustain. Chem. Eng.* **8**, 6826–6833 (2020).
25. Chien, A. T., Cho, S., Joshi, Y. & Kumar, S. Electrical conductivity and Joule heating of polyacrylonitrile/carbon nanotube composite fibers. *Polymer* **55**, 6896–6905 (2014).
26. Luong, D. X. et al. Gram-scale bottom-up flash graphene synthesis. *Nature* **577**, 647–651 (2020).
27. Lu, M. et al. Continuous stabilization of polyacrylonitrile (PAN)-carbon nanotube (CNT) fibers by Joule heating. *Chem. Eng. Sci.* **236**, 116495 (2021).
28. Sarmah, A. et al. Recycle and reuse of continuous carbon fibers from thermoset composites using Joule heating. *ChemSusChem* **15**, e202200989 (2022).
29. Cheng, Y. et al. Electric current aligning component units during graphene fiber Joule heating. *Adv. Funct. Mater.* **32**, 2103493 (2022).
30. Nguyen, S. et al. Characterizing Joule heating effects on single suspended carbon fibers: calculating the temperature coefficient of resistance for localized carbon nanotube growth. *J. Phys. Chem. C* **128**, 12593–12603 (2024).
31. Lu, S., Song, P., Harper, L. & Turner, T. Joule heating of carbon fibre tapes—a low-cost approach for automated dry fibre deposition. *Compos. A* **187**, 108498 (2024).
32. Warren, C. D. *Low Cost Carbon Fiber Overview* (Oak Ridge National Laboratory, 2011).
33. Das, S. Life cycle assessment of carbon fiber-reinforced polymer composites. *Int. J. Life Cycle Assess.* **16**, 268–282 (2011).
34. Sharma, R., Ravikumar, N. L., Dasgupta, K., Chakravartty, J. K. & Kar, K. K. in *Composite Materials: Processing, Applications, Characterizations* (ed. Kar, K.) 315–367 (Springer, 2017).
35. Song, Q., Li, K., Li, H. & Fu, Q. Increasing the tensile property of unidirectional carbon/carbon composites by grafting carbon nanotubes onto carbon fibers by electrophoretic deposition. *J. Mater. Sci. Technol.* **29**, 711–714 (2013).
36. Yin, X. et al. Recent progress in 1D nanostructures reinforced carbon/carbon composites. *Adv. Funct. Mater.* **32**, 2204965 (2022).
37. Salim, N. V. et al. The role of tension and temperature for efficient carbonization of polyacrylonitrile fibers: toward low cost carbon fibers. *Ind. Eng. Chem. Res.* **57**, 4268–4276 (2018).
38. Jacob, R. J., Kline, D. J. & Zachariah, M. R. High speed 2-dimensional temperature measurements of nanothermite composites: probing thermal vs. Gas generation effects. *J. Appl. Phys.* **123**, 115902 (2018).
39. Wang, X. et al. Continuous 2000 K droplet-to-particle synthesis. *Mater. Today* **35**, 106–114 (2020).
40. Der, A. et al. Modelling and analysis of the energy intensity in polyacrylonitrile (PAN) precursor and carbon fibre manufacturing. *J. Clean. Prod.* **303**, 127105 (2021).
41. Bare, J. C., Norris, G. A., Pennington, D. W. & McKone, T. TRACI–the tool for the reduction and assessment of chemical and other environmental impacts. *J. Ind. Ecol.* **6**, 49–78 (2003).

Acknowledgements

The project was funded by the Advanced Research Projects Agency-Energy (ARPA-E), US DOE, under award no. DE-AR0001191 to L.H., S.K., Chao Wang and P.L. This research used resources of the Centre for Functional Nanomaterials (CFN), which is a US DOE Office of Science User Facility, at Brookhaven National Laboratory under contract no. DE-SC0012704. S.K. and C.A.W. acknowledge the use of facilities in part at the Georgia Tech Institute for Electronics and Nanotechnology, a member of the National Nanotechnology Coordinated Infrastructure (NNCI), which is supported by the National Science Foundation (ECCS-2025462). L.H. and T.L. acknowledge the use of facilities at the Maryland NanoCentre.

Author contributions

L.H. and T.L. designed the CH_4 upgrading experiments. T.L. developed the upgrading setup, upgraded all CFs and conducted performance measurement, materials characterization and cost and thermal analyses. K.Z. and Q.D. performed the upgrading process optimization and materials analysis. X. Zhao carried out thermal analysis and calculations. X. Zhang conducted materials characterization. X.W. performed temperature tests during Joule heating. Chao Wang analysed the process of hydrocarbon pyrolysis and materials structure. H.Z. and Canhui Wang performed the high-resolution electron microscopy. S.K. and K.G. developed the setup for spinning and carbonization. C.A.W., B.J., P.J.A.-M. and K.J.M. performed precursor fibre spinning, carbonization and related characterization. P.L. offered the cost model. M.G. and S.W. did the cost analyses. H.G. conducted the comparative LCA. D.L. provided reactor design and optimization. S.C. measured and calculated the methane conversion rate and hydrogen yield. T.L. and A.H.B. collectively wrote the paper with inputs from all authors. All authors commented on the final paper.

Competing interests

L.H., S.K., Chao Wang, T.L., Canhui Wang, Q.D., B.J., P.J.A.-M. and K.G. have a US Patent Cooperation Treaty (PCT) patent application (no. 63/191,917) related to this work. L.H., S.K., Canhui Wang, Chao Wang and K.G. received an ARPA-E Plus Up grant to create a startup company, Carbon Plus, for commercialization. The other authors declare no competing interests.

Additional information

Supplementary information The online version contains supplementary material available at https://doi.org/10.1038/s41893-026-01815-w.

Correspondence and requests for materials should be addressed to Satish Kumar, Chao Wang or Liangbing Hu.

Peer review information *Nature Sustainability* thanks Agnieszka Brandt-Talbot, Jonggeol Na and the other, anonymous, reviewer(s) for their contribution to the peer review of this work.

Reprints and permissions information is available at www.nature.com/reprints.

Publisher's note Springer Nature remains neutral with regard to jurisdictional claims in published maps and institutional affiliations.

[1]Department of Electrical & Computer Engineering, Yale University, New Haven, CT, USA. [2]Department of Materials Science and Engineering, University of Maryland, College Park, MD, USA. [3]Department of Chemical and Biomolecular Engineering, Johns Hopkins University, Baltimore, MD, USA. [4]Carbon Plus Inc., Ellicott City, MD, USA. [5]School of Materials Science and Engineering, Georgia Institute of Technology, Atlanta, GA, USA. [6]Department of Nanoengineering, University of California, San Diego, La Jolla, CA, USA. [7]Department of Chemical and Biomolecular Engineering, University of Delaware, Newark, DE, USA. [8]USDA Forest Service, Forest Products Laboratory, Madison, WI, USA. [9]Ralph O'Connor Sustainable Energy Institute, Johns Hopkins University, Baltimore, MD, USA. [10]Center for Materials Innovation, Yale University, New Haven, CT, USA. [11]Department of Materials Science, Yale University, New Haven, CT, USA. [12]These authors contributed equally: Tangyuan Li, Canhui Wang, Cliff A. Wood, Kaizhu Zeng. ✉e-mail: satish.kumar@mse.gatech.edu; chaowang@jhu.edu; liangbing.hu@yale.edu

nature portfolio

Corresponding author(s): Liangbing Hu

Last updated by author(s): Feb 4, 2026

Reporting Summary

Nature Portfolio wishes to improve the reproducibility of the work that we publish. This form provides structure for consistency and transparency in reporting. For further information on Nature Portfolio policies, see our Editorial Policies and the Editorial Policy Checklist.

Statistics

For all statistical analyses, confirm that the following items are present in the figure legend, table legend, main text, or Methods section.

n/a	Confirmed	
☐	☒	The exact sample size (*n*) for each experimental group/condition, given as a discrete number and unit of measurement
☐	☒	A statement on whether measurements were taken from distinct samples or whether the same sample was measured repeatedly
☒	☐	The statistical test(s) used AND whether they are one- or two-sided *Only common tests should be described solely by name; describe more complex techniques in the Methods section.*
☐	☒	A description of all covariates tested
☐	☒	A description of any assumptions or corrections, such as tests of normality and adjustment for multiple comparisons
☐	☒	A full description of the statistical parameters including central tendency (e.g. means) or other basic estimates (e.g. regression coefficient) AND variation (e.g. standard deviation) or associated estimates of uncertainty (e.g. confidence intervals)
☒	☐	For null hypothesis testing, the test statistic (e.g. *F*, *t*, *r*) with confidence intervals, effect sizes, degrees of freedom and *P* value noted *Give P values as exact values whenever suitable.*
☒	☐	For Bayesian analysis, information on the choice of priors and Markov chain Monte Carlo settings
☐	☒	For hierarchical and complex designs, identification of the appropriate level for tests and full reporting of outcomes
☒	☐	Estimates of effect sizes (e.g. Cohen's *d*, Pearson's *r*), indicating how they were calculated

Our web collection on statistics for biologists contains articles on many of the points above.

Software and code

Policy information about availability of computer code

Data collection	SimaPro Craft v.10.1.0.6 software (incorporating the primary U.S. Life Cycle Inventory Database) used for life cycle assessment evaluation of carbon fiber production.
Data analysis	ImageJ v1.53e software used for measuring the diameter, cross-sectional area, and pore area in SEM images of fiber cross-sections; Adobe Illustrator 2021 and OriginLab software used for figure preparation.

For manuscripts utilizing custom algorithms or software that are central to the research but not yet described in published literature, software must be made available to editors and reviewers. We strongly encourage code deposition in a community repository (e.g. GitHub). See the Nature Portfolio guidelines for submitting code & software for further information.

Data

Policy information about availability of data

All manuscripts must include a data availability statement. This statement should provide the following information, where applicable:

- Accession codes, unique identifiers, or web links for publicly available datasets
- A description of any restrictions on data availability
- For clinical datasets or third party data, please ensure that the statement adheres to our policy

The data that support the findings of this study are available in this paper and its Supplementary Information. Source data are provided with this paper.

Human research participants

Policy information about studies involving human research participants and Sex and Gender in Research.

Reporting on sex and gender	*Use the terms sex (biological attribute) and gender (shaped by social and cultural circumstances) carefully in order to avoid confusing both terms. Indicate if findings apply to only one sex or gender; describe whether sex and gender were considered in study design whether sex and/or gender was determined based on self-reporting or assigned and methods used. Provide in the source data disaggregated sex and gender data where this information has been collected, and consent has been obtained for sharing of individual-level data; provide overall numbers in this Reporting Summary. Please state if this information has not been collected. Report sex- and gender-based analyses where performed, justify reasons for lack of sex- and gender-based analysis.*
Population characteristics	*Describe the covariate-relevant population characteristics of the human research participants (e.g. age, genotypic information, past and current diagnosis and treatment categories). If you filled out the behavioural & social sciences study design questions and have nothing to add here, write "See above."*
Recruitment	*Describe how participants were recruited. Outline any potential self-selection bias or other biases that may be present and how these are likely to impact results.*
Ethics oversight	*Identify the organization(s) that approved the study protocol.*

Note that full information on the approval of the study protocol must also be provided in the manuscript.

Field-specific reporting

Please select the one below that is the best fit for your research. If you are not sure, read the appropriate sections before making your selection.

☐ Life sciences ☐ Behavioural & social sciences ☒ Ecological, evolutionary & environmental sciences

For a reference copy of the document with all sections, see nature.com/documents/nr-reporting-summary-flat.pdf

Ecological, evolutionary & environmental sciences study design

All studies must disclose on these points even when the disclosure is negative.

Study description	In this study, we develop an electrified carbon fiber upgrading approach to fabricate low-cost CB(carbon black)/PAN(polyacrylonitrile) CFs(carbon fibers) by utilizing cost-effective and eco-friendly methane (CH4)-derived carbon (including CB and carbon deposited from CH4 pyrolysis). We first prepared CB/PAN CFs composed of CB and PAN using dry-jet wet spinning and furnace heating to produce a porous microstructure composed of aligned fibril networks. We then used these porous fibers as a Joule heating element in the presence of CH4. The porous microstructure facilitates CH4 diffusion throughout the pores, while the Joule heating process generates high temperatures that promote carbon deposition from CH4 pyrolysis as well as structure densification and carbonization, leading to improved mechanical and electrical properties of the CB/PAN CFs.
Research sample	Poly(acrylonitrile-co-methacrylic acid) (PAN, 4 wt% copolymers) of 500,000 g/mol molecular weight was used as the polymer binder and obtained from Japan Exlan Co. (Osaka, Japan). Dimethylformamide (DMF, ACS grade, 99.8%) was obtained from Sigma-Aldrich. Thermal carbon black (CB, Commercial Thermax® N991, Cancarb Limited, Canada; produced by the thermal decomposition of high purity methane feedstock) of 200 nm–400 nm in diameter was derived from conventional methane pyrolysis. Methane (ultra-high purity grade, ME UHP300) and argon (ultra-high purity grade, AR UHP300) were purchased from Airgas.
Sampling strategy	To prepare the CB/PAN solutions of different CB sizes/contents, the CB was first dispersed in DMF via 24 h sonication at a concentration determined by the target solid content. The CB/PAN solutions were then prepared by mixing dried PAN with the chilled (273 K) CB/DMF solution for 1 h, followed by increasing the temperature to 343 K and further stirring. Dry-jet wet spinning was conducted on a single filament system designed by Hills Inc., in which the CB/PAN solutions were extruded through a spinneret hole (e.g., 200 µm) into an air gap of 3 cm to 5 cm, followed by a coagulation bath of methanol and dimethyl acetamide (70/30 v/v). Stabilization of the CB/PAN precursor fibers was performed in a tube furnace (MHI H17HT2.5x24, Micropyretics Heaters International) in air atmosphere and heating at 530 K for 20 min. Carbonization was then performed in a tube furnace by heating the fiber bundle in a nitrogen atmosphere from room temperature to 1588 K at a rate of 5 K min-1. The carbonized CFs were used in the upgrading process by Joule heating.
Data collection	T. L. developed the upgrading setup, upgraded all carbon fibers, and conducted performance measurement, materials characterization, and cost and thermal analyses. K. Z. and Q. D. performed the upgrading process optimization and materials analysis. X. Z. carried out thermal analysis and calculation. X. Z. conducted materials characterization. X. W. performed temperature tests during Joule heating. C. W. analysed the process of hydrocarbon pyrolysis and materials structure. H. Z. and C. W. performed the high-resolution electron microscopy. S. K. and K. G. developed the setup of spinning and carbonization and directed the spinning, carbonization, and related characterization. C. W., B. J., P. A.-M., and K. M. performed precursor fiber spinning, carbonization, and related characterization. P. L. offered the cost model. M. G. and S. W. did the cost analyses. H. G. conducted the comparative LCA for this study. D. L. provided reactor design and optimization. S. C. measured and calculated the methane conversion rate and hydrogen yield.

Timing and spatial scale	Data collection occurred from January 2021 to May 2025. No significant differences in fiber morphology, structure, or performance were observed across different synthesis batches.
Data exclusions	No data were excluded from the analysis.
Reproducibility	All attempts to repeat the experiment were successful.
Randomization	All samples were tested randomly.
Blinding	There is no blinding in data collection in our work, as it does not involve ecological or medical experiments.

Did the study involve field work? ☐ Yes ☒ No

Reporting for specific materials, systems and methods

We require information from authors about some types of materials, experimental systems and methods used in many studies. Here, indicate whether each material, system or method listed is relevant to your study. If you are not sure if a list item applies to your research, read the appropriate section before selecting a response.

Materials & experimental systems

n/a	Involved in the study
☒	☐ Antibodies
☒	☐ Eukaryotic cell lines
☒	☐ Palaeontology and archaeology
☒	☐ Animals and other organisms
☒	☐ Clinical data
☒	☐ Dual use research of concern

Methods

n/a	Involved in the study
☒	☐ ChIP-seq
☒	☐ Flow cytometry
☒	☐ MRI-based neuroimaging